MRS Advances
https://doi.org/10.1557/s43580-025-01172-4

ORIGINAL PAPER

Raman spectroscopy study of the influence of additives (Cr-, Cr/Al-, and Gd) on UO_2 dissolution behavior

A. Milena-Pérez[1,2] · L. J. Bonales[1] · N. Rodríguez-Villagra[1] · J. Cobos[3] · H. Galán[1]

Received: 20 November 2024 / Accepted: 28 January 2025

Abstract

In this work, Raman spectroscopy (RS) has been used to study the behavior of spent nuclear fuel (SNF) under disposal conditions. In particular, evolutionary Accident-Tolerant Fuels (ATFs) consisting in UO_2 doped with Cr and Cr/Al; as well as neutron absorbers (UO_2 doped with Gd), has been manufactured and studied. The prepared pellets have been exposed to three different pH leachants (inert media, carbonated media, and young cement water with calcium) for distinct times. RS analyses have been conducted in both the leached and the unleached pellets. The results show that the addition of Cr, and Cr/Al does not lead to a noteworthy change of the pellet surface under the three media considered. Gd doping induces a higher intensity of the so-called "defects band," which is not dramatically affected after leaching. No secondary phases have been observed. These results are in good agreement with previous studies by XRD and SEM, thus validating RS as an accurate analytical technique.

Introduction

Raman spectroscopy (RS) is commonly known as a molecule identification and quantification technique with many outstanding advantages, such as no sample modification, no need of sample preparation, and low amount of sample required [1]. More importantly for the purpose of this study, RS has greatly evolved since its discovery in 1928 [2], making it possible nowadays to use this technique not only in the laboratory with sophisticated high-precision equipment, but also to develop field equipment for in situ analysis and on line monitoring of different processes. Moreover, this technique, envisioned as a stand-off technique (Raman spectra acquired where the spectrometer, and therefore the operator, is at some distance from the sample under analysis [3]), allows the measurement of dangerous samples, such as explosives or nuclear fuel, while maintaining safety criteria, of a paramount importance for the operator´s safety [4].

In the nuclear field, RS has been used for studying the behavior of Spent Nuclear Fuel (SNF) under dry conditions. In these studies, SNF surrogates (both UO_2 [5, 6] and doped UO_2 [7, 8]) have been analyzed by RS, in oxidizing environments, mimicking some operations at the dry storage facility. Under these conditions, the SNF matrix (*i.e.,* UO_2) could undergo oxidation and form a number of uranium oxides, to finally reach U_3O_8, a phase with important implications in the fuel integrity [9]. The obtained spectral fingerprints of these oxides was used to identify them by in situ experiments performed at different conditions of temperature and oxygen availability [6]. For doing so, dedicated measurement protocols were optimized and successfully applied in the study of irradiated fuel in hot cells [10].

Beyond dry storage, it is accepted that after a number of stages in the back-end of the nuclear fuel cycle, SNF will be stored in a deep geological repository (DGR) [11]. The main concern in this repository is the potential release of radionuclides when groundwater contact the SNF. Once uranium reaches its solubility limit in groundwater, it can form uranyl secondary phases. Some of those phases may retain the released radionuclides, and retard their mobility and migration to the biosphere [11–13]. Although Raman spectra of the different possible secondary phases are known both experimentally [14] and simulated [15], the use of RS to analyze fuel dissolution and formation of these phases

✉ N. Rodríguez-Villagra
Nieves.rodriguez@ciemat.es

[1] Centro de Investigaciones Energéticas, Medioambientales y Tecnológicas (CIEMAT), Av. Complutense, 40, 28040 Madrid, Spain

[2] Studsvik Nuclear AB, 61182 Nyköping, Sweden

[3] Estación Biológica de Doñana (EBD-CSIC), Avda. Américo Vespucio 26, 41092 Seville, Spain

Published online: 04 February 2025

is scarce in the literature and limited to UO_2 [16] or MOX fuel [17].

In this work, we propose going one-step further, using RS to study the dissolution behavior of Accident-Tolerant Fuels (ATFs). ATFs have emerged as a promising advancement to improve the safety and performance of nuclear reactors. Designed to withstand higher temperatures and to reduce the release of radioactive fission products, ATFs are engineered to have enhanced material properties compared to conventional UO_2 fuel. One of the shortest-term concepts is doping conventional UO_2 fuels with different elements. These additive-based UO_2 fuels incorporate small quantities of metal oxides, primarily chromia (Cr_2O_3) or chromia-alumina (Cr_2O_3–Al_2O_3) [18–20]. Besides ATFs, one widely researched type of doped nuclear fuel includes UO_2 doped with small amounts of gadolinium oxide (Gd_2O_3) because it acts as a Burnable Neutron Absorber (BNA) that helps managing reactivity within the reactor core [21].

The behavior of SNF in DGR environments is influenced by the chemical and physical properties of groundwater, including pH, complexing agents, and redox conditions. The UO_2 typically undergoes oxidative dissolution when exposed to oxygenated water or some anionic species that promote complexation (*e.g.,* bicarbonates) [22]. The presence of certain dopants may affect the solubility, surface reactivity, and the formation of secondary phases during the corrosion process [23]. Preliminary data on doped UO_2 suggests that its corrosion behavior under repository conditions is similar to undoped UO_2 at neutral and basic pH levels, but differences occur in high-carbonate environments or under mildly oxidizing conditions [24]. These variations are associated to the dopants that alter surface properties, influencing the dissolution rates that influence overall fuel stability. By understanding how dopants affects the behavior of UO_2 under repository conditions, experiments on the stability of SNF should be refined, supporting in the design of safer and more efficient nuclear waste management strategies. One approach of refining these experiments is to monitor in situ the behavior of these fuels under controlled conditions approximating DGR environments, such as groundwater compositions. Prior to this type of in situ studies, here we examine the surface alteration of doped UO_2 fuels by analyzing leached doped fuel pellets using RS, and comparing the Raman data obtained with the same unleached pellets. In addition to Raman investigations, the fuel samples studied here have been also analyzed by X-Ray Diffraction (XRD) and Scanning Electron Microscope (SEM), both prior and after the same leaching experiments. The results of such study can be found in a recently published study [25].

Materials and methods

Samples studied in this work consisted in doped pellets: UO_2-0.06 wt% Cr_2O_3, UO_2-0.05 wt% Cr_2O_3-0.02 wt% Al_2O_3, and UO_2-4.5 wt% Gd_2O_3. The materials were obtained by following a conventional solid-state sintering process. UO_2 (provided by ENUSA) and high-purity dopants (Cr_2O_3, Al_2O_3, and Gd_2O_3, provided by Alfa-Aesar) were mixed in weighted proportions to obtain the desired stoichiometry. Each powder mix was subjected to mechanical uniaxial pressing at 700 MPa to produce the green pellets. Those were first calcined at three temperatures (100, 300, and 500 °C) and then sintered at 1675 °C in a reducing atmosphere (4.7% H_2/N_2). Sintered pellets were then polished and finally etched (at 90% of the sintering temperature in 4.7% H_2/N_2 atmosphere) to reveal the grain structure. A more detailed description can be found in a previous study [25].

Dissolution tests were performed using three leaching solutions (300 mL): (a) inert media (labeled as PC, 20 mM $NaClO_4$, pH = 7.2); (b) carbonated media (identified as BC, 19:1 mM of $NaHCO_3$:NaCl, pH = 8.9); and (c) young cement water with calcium (named YCW, pH ~ 13.5 and simulating hyperalkaline conditions with calcium). Static dissolution tests were performed in an Ar glove box using autoclaves under 4.7%H_2-N_2 gas ($pH_2 = 0.37 \pm 1$ bar) at 22 ± 3 °C. Each doped UO_2 sample was exposed to leachants for 136 days (PC), 168 days (BC), and 379 days (YCW), respectively. Details of the leachant preparation in the laboratory and leaching experiment results are given elsewhere [25].

Both, the as-prepared sintered and the post-leached pellets were analyzed in detail by RS (Horiba LabRam HR evolution spectrometer, Jobin Yvon Technology, using a He–Ne laser with an excitation wavelength of 632.8 nm). Each spectra represents the averaged spectra from ten individual spectrums recorded at random locations of each disk. Raman data analysis has consisted in (1) calculating the exact position of the Raman features by using the second derivative method [5], and (2) using these positions as input parameters in the profile analysis, performing the fitting of the data with Lorentzian functions and calculating the intensity of each band. Uncertainty of the band´s positions has been calculated as the standard deviation of the 10 individual spectra. In the case of the intensity ratios, the uncertainty analysis has been done by error propagation from the uncertainty obtained in every individual fitting.

Results and discussion

Figures 1, 2 and 3 show the averaged Raman spectra acquired from the surface of the unleached pellets of Cr-, Cr/Al-, and Gd-doped UO_2, respectively, and after being

immersed in PC, BC, and YCW. The Raman spectra of the as-prepared materials (Figs. 1a, 2a, 3a) show the typical UO_2 Raman spectrum, containing some features consistent with the literature [5, 8, 26]: (a) 445 cm^{-1} (T_{2g}), corresponding to the vibration of the U–O bond within the UO_2 matrix; (b) 575 cm^{-1} (LO phonon) associated with the presence of defects in the fluorite lattice; and (c) ~ 1140 cm^{-1} (2LO), representing the first overtone of this phonon vibration. In the case of UO_2 matrices doped with trivalent elements, as in this work, the substitution of U(IV) by M(III) (M = Cr, Al or Gd) creates a charge imbalance in the lattice. On the one hand, this imbalance is compensated by the creation of oxygen vacancies, as recently demonstrated by Murphy et al. [27]studying Cr-doped UO_2 fuel by Electron Paramagnetic Resonance. On the other hand, the compensation proceeds through the creation of U(V), as proposed by Kim et al. [28] in their study about the air-oxidation of Gd-doped UO_2 and recently confirmed by Vinograd et al. [29]. In any case, Raman spectroscopy is sensitive to the creation of these defects in the lattice, by the appearance of a broad band around 540 cm^{-1} in the spectra [7, 30]). Often, both this band at 540 cm^{-1} and the LO phonon at 575 cm^{-1} overlap, giving place to a broad band generally known as "defects band" [31]. For the sake of simplicity, this feature is named as "LO" in ulterior analyses and plots. These modes give a very good estimation of the sensitivity of RS to the amount of dopant that has entered into the UO_2 matrix. In Figs. 1a, 2a, the intensity of this band is quite low (with intensity values around 0.2, Figs. 1c and 2c). However, in the case of Gd-doped UO_2, it can be seen that the band is much more intense (Fig. 3a), with an intensity value of around 3.7 (Fig. 3c). This behavior is explained by the higher solubility of Gd in the solid solution with UO_2, compared to Cr and Al [7].

Regarding the Raman spectra of the leached samples, they are also shown in Figs. 1 to 3. As a general comment, no uranyl secondary phases were identified on the surface for the three doped UO_2 pellets. The presence of secondary phases, such as studtite ($UO_4{\cdot}2H_2O$) or schoepite ($(UO_2)(OH)_2{\cdot}xH_2O$) on the surface of UO_2 leads to additional Raman bands in the region of 700–900 cm^{-1} [32], which are not observed here. In the following paragraphs, a detailed description of the behavior of each one of the

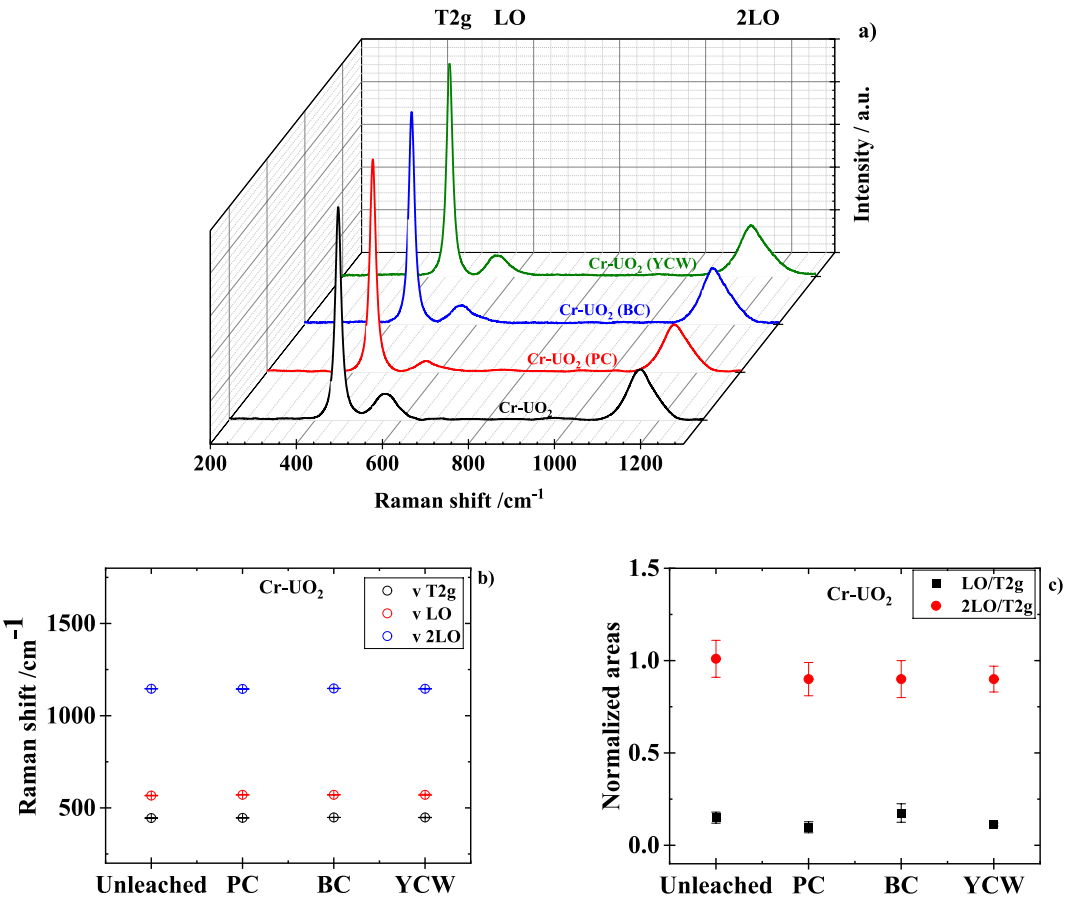

Fig. 1 **a** Comparison of the Raman spectra on Cr-doped UO_2 pellets: unleached (black) and after immersed in PC (red), BC (blue), and YCW (green) solutions; **b** position of T_{2g}, LO, and 2LO as a function of leachant; and **c** peak area ratio of LO/T_{2g} and 2LO/T_{2g}

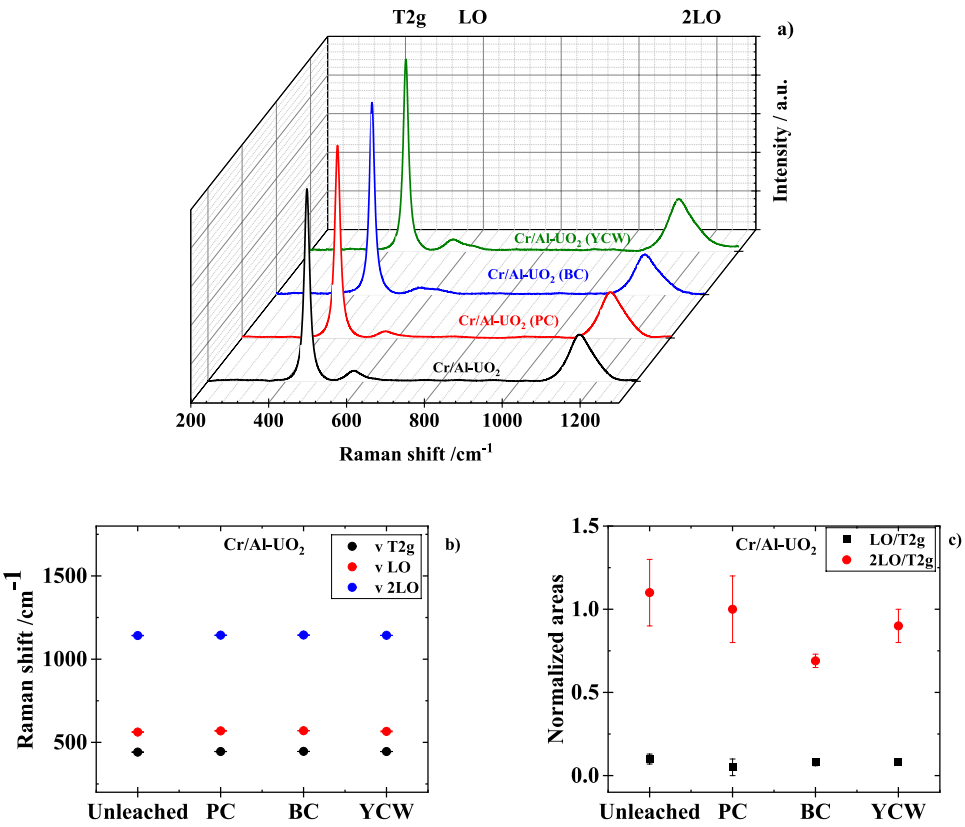

Fig. 2 **a** Comparison of the Raman spectra on Cr/Al-doped UO_2 pellets: unleached (black) and after immersed in PC (red), BC (blue), and YCW (green) solutions; **b** position of T_{2g}, LO, and 2LO as a function of leachant; and **c** peak area ratio of LO/T_{2g} and 2LO/T_{2g}

Raman modes described before for every doped material studied is presented.

From the analysis of Cr-UO_2 (Fig. 1b), it can be concluded that there is no significant changes from the three main band position, *i.e.,* T_{2g}, LO, and 2LO. The calculated areas of LO and 2LO bands normalized to that of the T_{2g} band are plotted against the leachant in Fig. 1c. The data of the 2LO/T_{2g} area ratios for leached pellets seems constant within error margins, but slightly decreased compared to the one of the unleached pellet, which may imply an increase in defects in the surface oxide. The change in the peak area ratios of 2LO/T_{2g} should instead be attributed to the chemical behavior of surface U atoms [33] as the dissolution process results in the formation of vacancies within the crystal structure.

The same analytical procedure was applied for the Cr/Al-UO_2 sample. Fig. 2a shows the Raman spectrum of Cr/Al-UO_2 prior and post-leached at pH 7.2, 8.9, and 13.5, where one can see the previously mentioned main features of UO_2. Fig. 2b shows the position the three main bands with no appreciable changes among unleached and leached Cr/Al-UO_2 samples. However, the position of the T_{2g} band is slightly deviated at lower frequencies (441 cm^{-1}) compared to the sample where Cr is the solely dopant (445 cm^{-1}). The normalized area of the LO and 2LO bands to T_{2g} (Fig. 2c) for leached sample in BC decreased compared to the pre-tested sample. The most notably drop corresponds to the 2LO/T_{2g} peaks ratio for sample leached in BC.

The Raman spectra of Gd-UO_2 significantly changes (Fig. 3a) compared to the previous untreated samples. While the relative intensity of the two bands at 445 cm^{-1} and 1150 cm^{-1} decreases, the broad band between 500 and 700 cm^{-1} increases. Consequently, the 2LO/T_{2g} ratio decreases (Fig. 3c) compared to Cr- and Cr/Al-UO_2 (Figs. 1c and 2c, respectively) possibly indicating more distortion for Gd, but the LO intensity increases with the doping level, as in this sample with 4.5%. This can be clearly observed when compared the LO/T_{2g} normalized area in Fig. 3c, with Figs. 1c and 2c for the as-sintered samples with lower amount of trivalent dopants. For this dopant, while the normalized area of the 2LO band remains almost the same, the area ratio of the LO band significantly increases at pH 7.2 and 8.9. On the contrary, it decreases at pH 13.5 (Fig. 3c) together with a broadening of the LO peak maybe caused by some surface oxidation. Anyhow, this potential oxidation, if any, should be very small, since there are no clear hints of the presence of the band related to the excess of oxygen in the lattice at around 630 cm^{-1} [5].

All the mentioned results from RS were also confirmed by XRD analysis on the leached surfaces [25]. These primary data from ex situ leached samples allow us continuing with in situ and/or *operando* experiments in order to provide

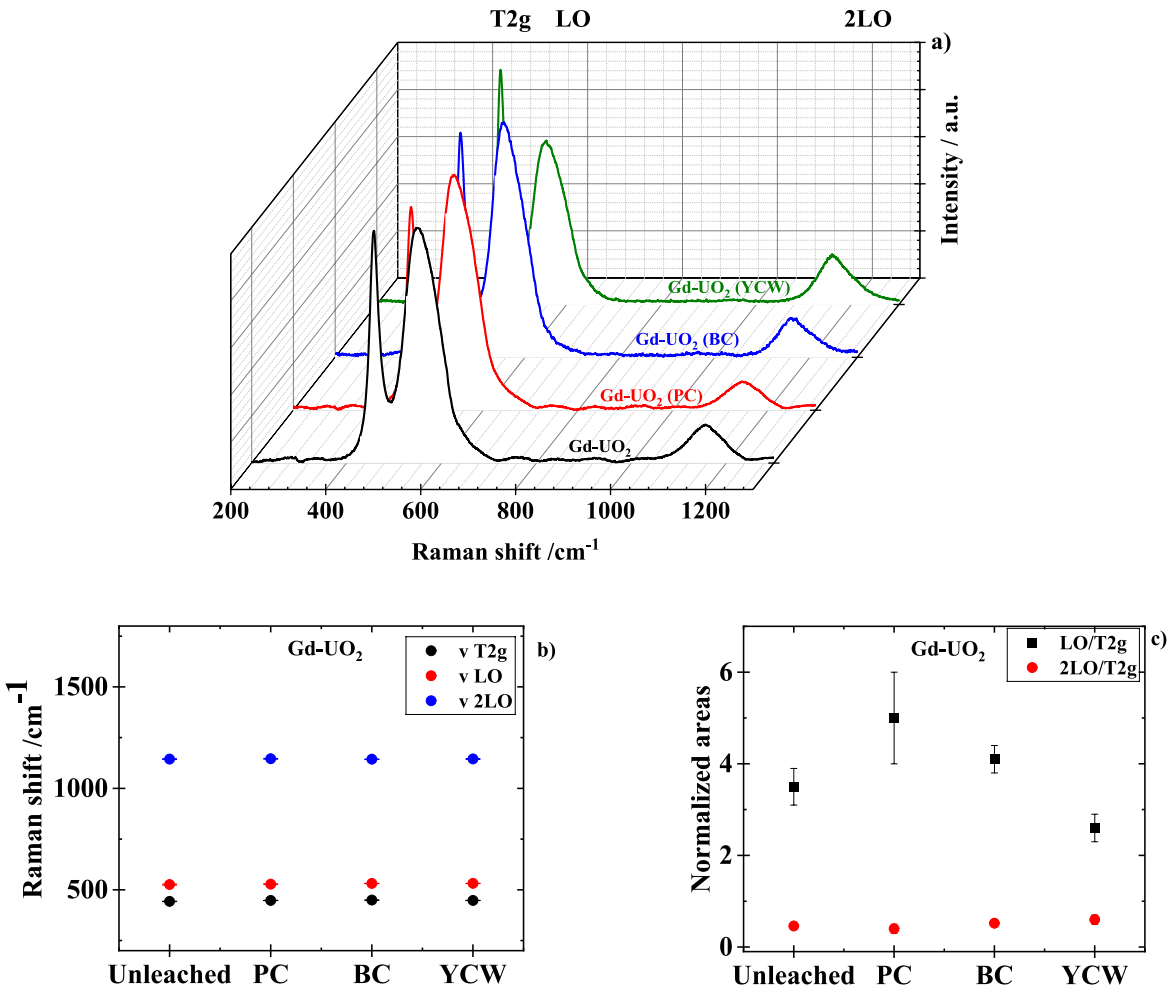

Fig. 3 **a** Comparison of the Raman spectra on Gd-doped UO_2 pellets: unleached (black) and after immersed in PC (red), BC (blue), and YCW (green) solutions; **b** position of T_{2g}, LO, and 2LO as a function of leachant; and **c** peak area ratio of LO/T_{2g} and $2LO/T_{2g}$

additional insights into the nuclear fuel behavior and the effect of dopants under different environments.

Conclusion

In this work we have demonstrated the capacity of Raman spectroscopy in the analysis of the dissolution of new fuels, such as ATFs (Cr- and Cr/Al-doped UO_2) and BNA (Gd-doped UO_2), in three different leachants at pH 7.2, 8.9, and 13.5, relevant in the context of SNF behavior in a deep geological repository. The results, in agreement with the ones obtained by XRD show that the addition of Cr, and Cr/Al does not lead to a noteworthy change of the pellet surface under the three media considered. The incorporation of 4.5 wt% of Gd_2O_3 doping induces a marked increase in the intensity of the so-called "defect band" (mainly attributed to the LO phonon associated with lattice disorder), because of defects formation caused by doping. The analyses of the leached samples surfaces by RS show the absence of precipitated secondary phases containing uranium. It can be inferred that RS is a suitable technique in the analysis of this type of experiments (prior and after the leaching test). The results obtained here open the door to explore the kinetic corrosion of doped UO_2 in groundwater using in situ conditions and RS as the monitoring technique.

Acknowledgments This work was funded by the European Commission Horizon 2020 Research and Training Programme, DISCO, of the European Atomic Energy Community (EURATOM), under grant agreement number 755443. We also wish to acknowledge funding from the Spanish State Research Agency (SRA), grant PID2021-124913OA-I00, IONMAT project funded by MCIN/AEI/ https://doi.org/10.13039/501100011033.

Author contributions AMP and LJB performed/analyzed the Raman spectra, and wrote the original draft. NRV conceived of the idea, performed the dissolution experiments and reviewed the work. JC and HG reviewed the findings of this work.

Funding Open Access funding provided thanks to the CRUE-CSIC agreement with Springer Nature. This work has been developed and funded by the European Commission Horizon 2020 Research and Training Programme, DISCO of EURATOM (grant agreement nº: 755443) and by the Spanish State Research Agency (SRA) IONMAT project (grant nº: PID2021-124913OA-I00) funded by MCIN/AEI/https://doi.org/10.13039/501100011033.

Data availability Data sets generated during the current study are available from the corresponding author on reasonable request.

Declarations

Competing interests The authors have no conflicts of interest to declare.

References

1. Raman spectroscopy applied to Earth sciences and cultural heritage: European Mineralogical Union, 2012
2. R.S. Krishnan, R.K. Shankar, Raman effect: History of the discovery. J. Raman Spectrosc. **10**, 1–8 (1981)
3. A.J. Hobro, B. Lendl, Stand-off Raman spectroscopy. TrAC Trends Anal. Chem. **28**, 1235–1242 (2009)
4. L.J. Bonales, J.M. Elorrieta, A. Lobato, J. Cobos, Raman spectroscopy, a useful tool to study nuclear materials, applications of molecular spectroscopy to current research in the chemical and biological sciences, in *Applications of molecular spectroscopy to current research in the chemical and biological sciences*, vol. 1, ed. by D.M. Stauffer (INTECH open science, London, 2016)
5. J.M. Elorrieta, L.J. Bonales, N. Rodriguez-Villagra, V.G. Baonza, J. Cobos, A detailed Raman and X-ray study of UO_{2+x} oxides and related structure transitions. Phys. Chem. Chem. Phys. **18**, 28209–28216 (2016)
6. A. Milena-Pérez, L.J. Bonales, N. Rodríguez-Villagra, H. Galán, Exploring the impact of temperature and oxygen partial pressure on the spent nuclear fuel oxidation during its dry management. Sci. Rep. **13**, 1966 (2023)
7. A. Milena-Pérez, L.J. Bonales, N. Rodríguez-Villagra, S. Fernández, V.G. Baonza, J. Cobos, Raman spectroscopy coupled to principal component analysis for studying UO_2 nuclear fuels with different grain sizes due to the chromia addition. J. Nucl. Mater. **543**, 152581 (2021)
8. J.M. Elorrieta, L.J. Bonales, S. Fernández, N. Rodríguez-Villagra, L. Gutiérrez-Nebot, V.G. Baonza et al., Pre-and post-oxidation Raman analysis of (U, Ce)O_2 oxides. J. Nucl. Mater. **508**, 116–122 (2018)
9. A. Milena-Pérez, N. Rodríguez-Villagra, F. Feria, C. Aguado, L.E. Herranz, Critical review of fuel oxidation database under dry storage conditions. Prog. Nucl. Energy **165**, 104914 (2023)
10. A. Milena-Pérez, L.J. Bonales, L. Emblico, D. Serrano-Purroy, N. Rodríguez-Villagra, Spent nuclear fuel oxidation under dry storage controlled conditions for studying its radial oxidation behavior. J. Nucl. Mater. **589**, 154831 (2024)
11. K. Spahiu, "State of the knowledge report—Spent nuclear fuel domain 3.1.1. EURAD—European Joint Programme on Radioactive Waste Management (847593)," 2021.
12. R.C. Ewing, Long-term storage of spent nuclear fuel. Nat. Mater. **14**, 252–257 (2015)
13. R. Finch, *Secondary uranium-phase paragenesis and incorporation of radionuclides into secondary phase* (US Department of Energy, Las vegas, 2001)
14. R.L. Frost, J. Čejka, A Raman spectroscopic study of the uranyl mineral rutherfordine—revisited. J. Raman Spectrosc. **40**, 1096–1103 (2009)
15. L.J. Bonales, F. Colmenero, J. Cobos, V. Timon, Spectroscopic Raman characterization of rutherfordine: a combined DFT and experimental study. Phys. Chem. Chem. Phys. **18**, 16575–16584 (2016)
16. R. Kusaka, Y. Kumagai, T. Yomogida, M. Takano, M. Watanabe, T. Sasaki et al., Distribution of studtite and metastudtite generated on the surface of U3O8: application of Raman imaging technique to uranium compound. J. Nucl. Sci. Technol. **58**, 629–634 (2021)
17. L. Sarrasin, S. Miro, C. Jégou, M. Tribet, V. Broudic, C. Marques et al., studtite formation assessed by Raman spectroscopy and 18O isotopic labeling during the oxidative dissolution of a MOX fuel. J. Phys. Chem. C **125**, 19209–19218 (2021)
18. J.C. Killeen, Fission gas release and swelling in UO_2 doped with Cr_2O_3. J. Nucl. Mater. **88**, 177–184 (1980)
19. J. Arborelius, K. Backman, L. Hallstadius, M. Limbäck, J. Nilsson, B. Rebensdorff et al., Advanced doped UO2 pellets in LWR applications. J. Nucl. Sci. Technol. **43**, 967–976 (2006)
20. A. Massih, "Effects of additives on uranium dioxide fuel behavior," Malmö högskola, School of Technology 2014.
21. IAEA, *Characteristics and Use of urania-gadolinia fuels* (International Atomic Energy Agency, Vienna, 1996)
22. M.E. Torrero, E. Baraj, J. de Pablo, J. Giménez, I. Casas, Kinetics of corrosion and dissolution of uranium dioxide as a function of pH. Int. J. Chem. Kinet **29**, 261–267 (1997)
23. A. Barreiro-Fidalgo, *Experimental studies of radiation-induced dissolution of UO2: The effect of intrinsic solid phase properties and external factors* (KTH Royal Institute of Technology, Stockholm, 2017)
24. A. Sjöland, P. Christensen, L.Z. Evins, D. Bosbach, L. Duro, I. Farnan et al., Spent nuclear fuel management, characterisation, and dissolution behaviour: progress and achievement from SFC and DisCo. EPJ Nucl. Sci. Technol. **9**, 13 (2023)
25. N. Rodríguez-Villagra, S. Fernández-Carretero, A. Milena-Pérez, L.J. Bonales, L. Gutierrez, J. Cobos et al., Impact of dopants and leachants on modern UO_2-based fuels alteration under final storage conditions: single and joint effects. J. Nucl. Mater. **606**, 155635 (2025). https://doi.org/10.1016/j.jnucmat.2025.155635
26. N. Liu, J. Kim, J. Lee, Y.-S. Youn, J.-G. Kim, J.-Y. Kim et al., Influence of Gd doping on the structure and electrochemical behavior of UO2. Electrochim. Acta **247**, 496–504 (2017)
27. G.L. Murphy, R. Gericke, S. Gilson, E.F. Bazarkina, A. Rossberg, P. Kaden et al., Deconvoluting Cr states in Cr-doped UO_2 nuclear fuels via bulk and single crystal spectroscopic studies. Nat. Commun. **14**, 2455 (2023)

28. J.G. Kim, Y.-K. Ha, S.-D. Park, K.-Y. Jee, W.-H. Kim, Effect of a trivalent dopant, Gd^{3+}, on the oxidation of uranium dioxide. J. Nucl. Mater. **297**, 327–331 (2001)
29. V.L. Vinograd, A.A. Bukaemskiy, G. Deissmann, G. Modolo, Thermodynamic model of the oxidation of Ln-doped UO2. Sci. Rep. **13**, 17944 (2023)
30. J. Lee, J. Kim, Y.-S. Youn, N. Liu, J.-G. Kim, Y.-K. Ha et al., Raman study on structure of $U_{1-y}Gd_yO_{2-x}$ (y=0.005, 0.01, 0.03, 0.05 and 0.1) solid solutions. J. Nucl. Mater. **486**, 216–221 (2017)
31. J.M. Elorrieta, A. Milena-Pérez, J.-F. Vigier, L.J. Bonales, N. Rodríguez-Villagra, New insights into the structural transition from UO2+x to U3O7 by quantitative Raman spectroscopy. Phys. Chem. Chem. Phys. **24**, 28394–28402 (2022)
32. F. Pointurier, D.H. Lin, D. Manara, O. Marie, T. Fanghänel, K. Mayer, Capabilities of micro-Raman spectrometry for the identification of uranium ore concentrates from analysis of single particles. Vib. Spectrosc. **103**, 102925 (2019)
33. J. McGrady, Y. Kumagai, M. Watanabe, A. Kirishima, D. Akiyama, S. Kimuro et al., A Raman spectroscopy study of bicarbonate effects on UO2+x. J. Nucl. Sci. Technol. **60**, 1586–1594 (2023)